J Solid State Electrochem (2016) 20:1149–1154
DOI 10.1007/s10008-015-2874-z

ORIGINAL PAPER

Insight into the electrochemical reduction of CO_2 on gold via surface-enhanced Raman spectroscopy and N-containing additives

Justin L. Oberst[1] · **Huei-Ru "Molly" Jhong**[1] · **Paul J. A. Kenis**[1,2] · **Andrew A. Gewirth**[1,2]

Received: 16 February 2015 / Revised: 24 April 2015 / Accepted: 27 April 2015 / Published online: 9 May 2015

Abstract Due to increasing levels of greenhouse gases in the atmosphere, increased attention has been given to minimizing their emissions and reducing current levels. Primarily focusing on CO_2, routes towards reducing atmospheric levels include capture, sequestration, and conversion. For CO_2 conversion, Au electrocatalysts have demonstrated high CO_2 reduction activity to CO which can then be further converted to various synfuels or commodity chemicals. In this work, we further probe Au electrocatalysts by utilizing a Ag-based model, using N-containing additives, such as pyrazole and benzotriazole, and surface-enhanced Raman spectroscopy. Surface-enhanced Raman spectroscopy (SERS) reveals that only in the presence of N-containing additives is a stronger CO band seen. These additives do not affect the CO_2 reduction mechanism of Au, as found by Tafel and product distribution analysis. We also demonstrate enhancement of the CO_2 reduction rate on Au by utilizing a known CO_2 scavenger, ethanolamine, adsorbed on the Au surface. This result suggests that improving CO_2 reduction should focus on the reactant side of the Sabatier plot.

Keywords CO_2 electroreduction · SERS · Additives · Mechanism · Electrocatalysis

Electronic supplementary material The online version of this article (doi:10.1007/s10008-015-2874-z) contains supplementary material, which is available to authorized users.

✉ Andrew A. Gewirth
agewirth@illinois.edu

[1] School of Chemical Sciences, University of Illinois at Urbana-Champaign, 600 S. Mathews Avenue, Urbana, IL 61801, USA

[2] International Institute for Carbon Neutral Energy Research (WPI-I2CNER), Kyushu University, Fukuoka, Japan

Introduction

Over the past several decades, greenhouse gas emissions have continuously increased. The detrimental environmental effect of these gases, most specifically CO_2, has led to intensive studies on their capture, sequestration, and conversion [1–4]. With respect to CO_2 conversion, captured CO_2 is reduced, using excess electricity, to CO or other various hydrocarbons. CO can then be reacted with H_2, a typical by-product in CO_2 reduction, in a water–gas shift reaction to form a variety of synfuels or commodity chemicals [2, 3]. Despite the intriguing nature of this process, CO_2 reduction is still limited by low energy efficiencies, partially due to high overpotentials required for conversion [2]. This issue drives much research towards the study and development of various CO_2 reduction catalyst/electrolyte systems and the interrogation of their reaction intermediates.

Depending on the electrocatalyst used, a wide variety of products can be obtained through the reduction of CO_2 in water [5]. For example, Cu-based catalysts form various hydrocarbons, including methane and ethylene [5–8]. Catalysts such as Pt, Ni, and Pd are poor CO_2 reducers due to strong binding and poisoning by the CO intermediate and form primarily H_2 in the potential window where CO_2 reduction occurs [5, 9]. In contrast, CO_2 reduction on Au and Ag demonstrates the highest Faradaic efficiencies for CO formation [5, 10]. For both Au and Ag, the higher activity compared to other metals is thought to be in part due to the weak binding of the CO product to the catalyst surface [9]. CO produced by Ag and Au catalysts can be collected and converted to various synfuels and commodity chemicals using a Fischer–Tropsch synthesis, utilizing any H_2 side product as well [3].

The electrochemical reduction of CO_2 by Au has been of high interest since Au exhibits the highest activity and selectivity for the conversion of CO_2 to CO [5, 9, 11]. Based on

studies of the kinetics of CO_2 reduction on Au, it has been proposed that the rate determining step is the conversion of CO_2 to CO_2^{*-} radical anion species [10, 12]. Attempts to further improve this reduction scheme have included altering the catalyst surface, to either stabilize reactants or destabilize products near the electrode surface, in order to decrease the applied overpotential and increase catalyst efficiency. In one example, a Au oxide nanoparticle has been synthesized that has improved Faradaic efficiencies, lower Tafel slopes, and higher exchange currents than that of polycrystalline Au [13]. However, the effect of the Au–O species on the reaction and intermediates remains little understood.

To understand CO_2 reduction on Au, vibrational spectroscopy has been frequently employed in a variety of systems, most being non-aqueous since these solvents are capable of dissolving more CO_2 than water. However, in some of these systems, Au loses product selectivity and can produce both CO and formic acid [14]. One such example, in a DMF solvent, Fourier transform infrared spectroscopy (FT-IR) and electron paramagnetic resonance (EPR) analysis were used to elucidate that CO_2 reduction proceeds, via the formation of free radicals, to form both CO and carbonate species [15]. In acetonitrile, in situ FT-IR was used to verify the production of CO, CO_3^{2-}, and formate [16]. To date, little work has been done in studying CO_2 reduction on Au in aqueous systems via vibrational spectroscopies, such as surface-enhanced Raman spectroscopy (SERS).

Previously, N-containing ligands, such as pyrazole (Pz) and 3,5-diamino-1,2,4-triazole (DAT), have been shown to result in an enhancement in electrocatalytic CO_2 conversion to CO when using a Ag-based electrocatalyst [17]. The Ag–DAT system was further interrogated in our group by utilizing SERS revealing that the presence of N-based additives may destabilize adsorbed CO leading to the enhancement of CO_2 conversion to CO based on the Sabatier principle [18]. In this work, we take inspiration from the Ag system and attempt to further interrogate the mechanism and limitations of CO_2 conversion on Au utilizing SERS and various N-containing additives, such as ethanolamine (EA) and Pz.

Experimental

Polycrystalline Au working electrodes (1 cm in diameter) were sequentially polished in 9-, 3-, 1-, and 0.25-μm diamond suspensions (MetaDi Supreme, Buehler). These electrodes were polished using the 0.25-μm suspension between studies. After polishing, the electrode was thoroughly rinsed using 18.2 MΩ Milli-Q water (Millipore Inc.). Electrochemical measurements were carried out in a two-compartment cell with a smooth Au electrode. Current densities were calculated using the geometric surface area of the Au disk (1 cm in diameter). For in situ SERS measurements, after polishing and rinsing, the Au electrode was then electrochemically roughened in a cell consisting of a Ag/AgCl (3 M KCl) reference electrode, a Au counter electrode, and a 0.5 M KCl electrolyte as previously described [19, 20]. The lower potential limit was −0.25 V vs. Ag/AgCl and the upper potential limit was 1.3 V vs. Ag/AgCl. Ten roughening cycles were carried out on the Au disk before use.

Electrolyte was 1 M KOH (99.99 % trace metal basis, Sigma-Aldrich) with a saturating concentration of $Ca(OH)_2$ (99.995 % metal basis, Sigma-Aldrich) prepared using Milli-Q water [18, 21]. In noted electrolytes, N-containing additives were added to achieve a 10-mM concentration. These compounds include 3,5-diamino-1,2,4-triazole (98 %, Aldrich), benzotriazole (99 %, Aldrich), pyrazole (98 %, Aldrich), and ethanolamine (99.5 %, Aldrich). Sparging the electrolyte with CO_2 effectively reduces the pH from approximately 13.1 to 7.8 [5]. For control experiments, the electrolyte was first sparged with Ar for 30 min and then the pH was adjusted using $HClO_4$ (Ultrex II Ultrapure Reagent grade, JT Baker). The electrolyte was sparged with Ar for an additional 30 to 60 min after the pH was adjusted.

Electrochemical experiments were carried out using a CHI760 potentiostat (CH Instruments). A Ag/AgCl "no leak" reference electrode (Cypress Systems) was used for all experiments. Potential conversion from "vs. Ag/AgCl" to "vs. reversible hydrogen electrode (RHE)" was completed by sparging an electrolyte with H_2 and measuring an open-circuit potential. For SERS measurements, a Pt wire was used as the counter electrode. For other electrochemical experiments, a Pt gauze counter electrode was used. Electrochemistry was carried out in a two-compartment cell with the counter electrode separated by the main compartment by a frit. Tafel analysis was carried out on iR-corrected Tafel plots. iR correction was achieved by measuring and subtracting the solution resistance as a function of potential.

In situ SERS measurements were carried out in a spectroelectrochemical cell previously described [22]. A 50-mW 632.8-nm He–Ne laser (Meredith Instruments) was used to excite the sample at an approximate 45° incident angle. Scattered radiation was collected using an f/1.2 collection lens (Canon) and focused to the 50-μm slit of a SpectraPro 2300i monochromator (Princeton Instruments). Using a grating with 1200 grooves/mm, the radiation was dispersed onto a CCD detector (Andor) that was cooled to −60 °C. Acquisition times for the spectra reported ranged from 10 to 30 s.

Results and discussion

Solution electrochemistry

Figure 1 shows voltammetry obtained from a Au electrode immersed in a pH=7.8 solution. The bare electrode

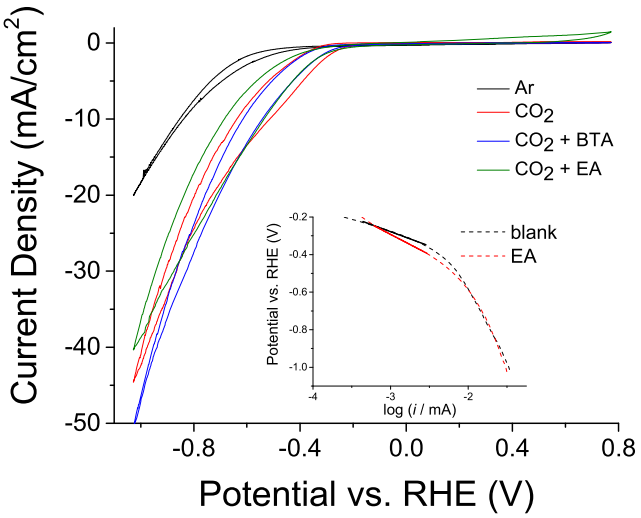

Fig. 1 Cyclic voltammetry (50 mV/s) of Au in 1 M KOH+$Ca(OH)_2$ (sat'd) under Ar (*black*) and under CO_2 (*red*) with 10 mM BTA (*blue*) and EA (*green*). Ar-saturated electrolytes had an adjusted pH of approximately 7.8. *Inset figure* shows Tafel analysis of Au in a CO_2-saturated electrolyte with (*red*) and without (*black*) EA

under Ar exhibits reductive current starting at −0.4 V associated with H_2 evolution. In the presence of CO_2 sparged into the electrochemical cell, the reductive current starts at −0.2 V; this reduction in onset is associated with CO_2 reduction. Prior work with Au has demonstrated that its primary product for CO_2 electroreduction is CO with a Faradaic efficiency of approximately 80 % for CO and less than 10 % for HCO_2^- and H_2 at reasonably low overpotentials [5, 6, 10, 11].

Figure 1 also shows the effect of addition of benzotriazole (BTA) on the CO_2 reduction onset. Addition of N-containing compounds such as BTA does not affect the voltammetry (Fig. 1) or product distribution (not shown) associated with CO_2 reduction to form CO. A similar insensitivity was seen for 3,5-diamino-1,2,4-triazole (DAT) and pyrazole (Pz). This behavior is in contrast to that found for Ag electrocatalysts, where addition of these N-containing ligands diminished the overpotential for CO formation by ca. 150 mV relative to catalysts not containing these species [17]. On Ag, the presence of the N-containing molecules was found to destabilize the product CO, yielding CO more weakly associated with the electrode surface [18]. Alternatively, CO is known to associate much less strongly with Au relative to Ag (ca. 0.40 eV vs. ca. 0.28 eV, respectively) [23–26]. The absence of this behavior on Au must mean that product destabilization is not operative on the Au surface through the addition of the N-containing molecules.

Figure 1 also shows the effect of addition of 10 mM of ethanolamine (EA) into the CO_2-containing electrolyte. EA is known to facilitate the capture of CO_2 by forming an EA carbamate when an EA solution is exposed to CO_2 [27]. Almost pure CO_2 can then be collected from the EA carbamate via reheating and the EA can be reused for CO_2 adsorption. The voltammetry shows that the overpotential for CO formation is diminished by ca. 35 mV when EA is present.

To further interrogate the effect these N-containing species on the mechanism of CO_2 reduction on Au, Tafel analyses on the low overpotential regions were completed. In the absence of N-containing additives, the Tafel slope is approximately 120 mV/decade, consistent with literature [10, 13, 28, 29]. Typically, on Au, Tafel slopes around 120 mV/decade indicate a rate determining step consisting of the first one-electron transfer to CO_2. The Tafel slope for CO_2 reduction in the presence of BTA is similarly found to be approximately 120 mV/decade. The similar current density, onset, and Tafel slope shows that BTA likely does not change the reaction mechanism on the Au electrode surface. Likewise, only modest changes in the Tafel behavior were found with addition of DAT or Pz (Supplemental Table 1).

Figure 1 shows that upon addition of EA to the CO_2-saturated electrolyte, the Tafel slope increases from ca. 120 mV/decade to ca. 220 mV/decade. High Tafel slopes in other systems are typically associated with several explanations including mass transfer limitations, a surface functionalized barrier, or a decreased number of active sites, perhaps due to H_2 or CO intermediate binding or N-containing additive adsorption in this case [30–33]. Tafel analysis was also completed on the high overpotential region revealing very high Tafel slopes. These will not be discussed in depth but are thought to be due to a combination of CO_2 reduction and hydrogen evolution (HER) which occurs at such negative potentials, as indicated by the cyclic voltammetry measured under Ar.

Raman spectroscopy

To further examine the effect of EA addition on the CO_2 reduction process and to contrast the behavior of other N-containing additives used to enhance CO_2 reduction on Ag surfaces, we performed SERS during the course of CO_2 reduction on Au [17, 18]. Figure 2 shows the potential dependence of the CO stretching vibration on a roughened Au electrode in the absence (a) and presence of Pz (b) and EA (c) in the bulk CO_2-saturated electrolyte. The peak at ca. 2120 cm^{-1} arises from CO adsorbed on Au at atop sites [34–36]. As seen in Fig. 2a, the CO stretching vibration is not seen on Au in the absence of N-containing compounds in solution. This behavior mimics prior reports demonstrating fluctuations of SER

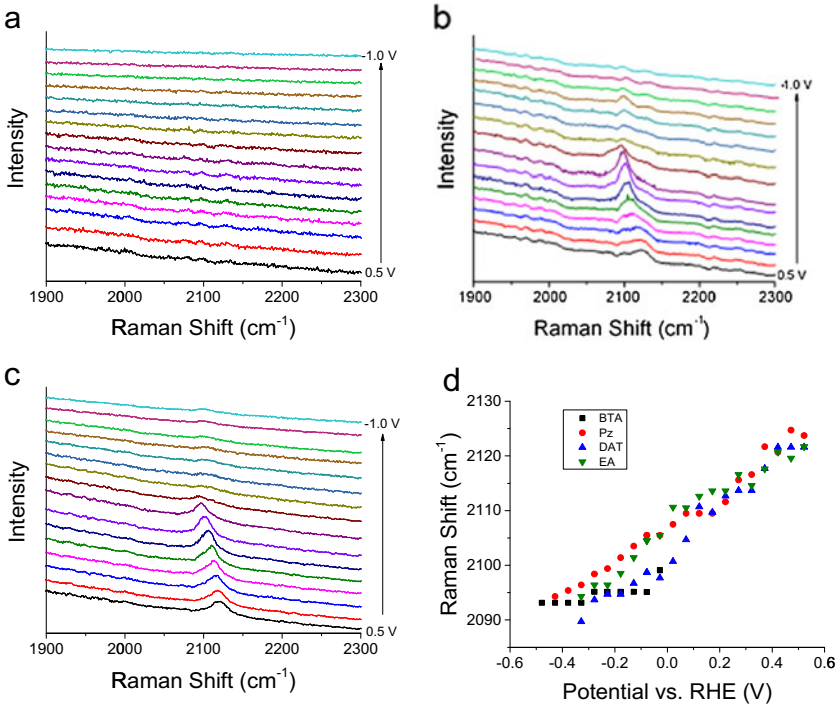

Fig. 2 SER spectra during cathodic sweep, at 0.1 V increments, in 1 M KOH+ $Ca(OH)_2$ (sat'd) electrolyte continuously sparged with CO_2 (**a**) with 10 mM Pz (**b**) and 10 mM EA (**c**). **d** shows the potential dependence of the CO stretching peak in the presence of each additive: BTA, Pz, DAT, and EA

spectra of CO on Au indicating surface restructuring of Au [34, 35]. When N-containing compounds, such as Pz and EA, are added to the electrolyte, the CO stretching band becomes evident as shown in Fig. 2b and c. This is also true for DAT and BTA, not shown. Also shown in Fig. 2d is the potential dependence on the CO stretching peak position. This peak shifts from ca. 2120 cm^{-1} at 0.4 V to ca. 2098 cm^{-1} at −0.4 V, prior to the peak disappearing at more negative potentials. This dependence yields a Stark shift of 32.1, 39.8, and 32.9 cm^{-1} V^{-1} for Pz, DAT, and EA, respectively. This value is consistent with the ca. 40 cm^{-1} V^{-1} found in literature for the Stark shift of the CO stretch [36–38].

Figure 3 shows the potential dependent SER spectra obtained from a roughened Au electrode in pH-adjusted Ar-saturated electrolytes with BTA (a), Pz (b), and EA (c). Compared with the spectra collected under CO_2 (Figure S1), the Ar-saturated spectra evince intense bands related to the added N-containing compounds at potentials close to open circuit [39, 40]. As the potential is swept more negative, the bands associated with the N-containing compounds slowly decrease in intensity before disappearing completely around −0.4 V. No features are evident in the CO stretching region (not shown). This behavior suggests that the N-containing compounds desorb at negative potentials, a behavior found on Ag as well [18].

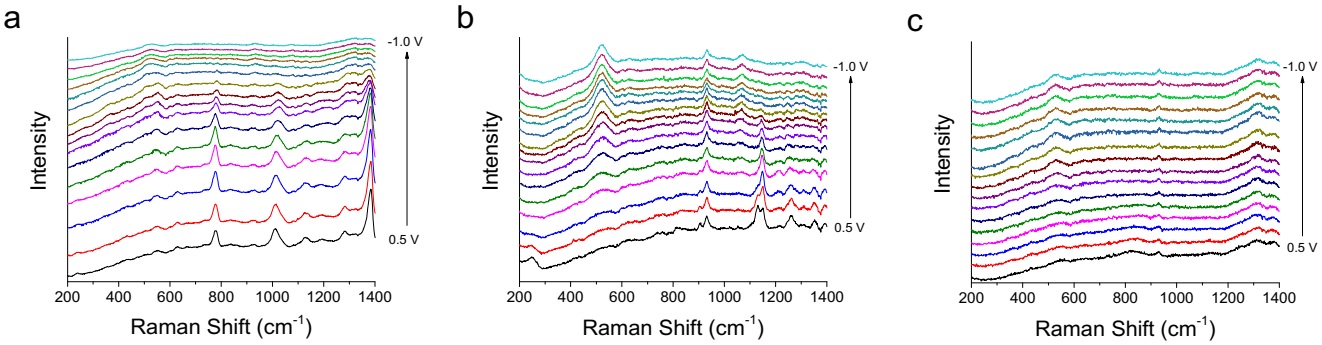

Fig. 3 SER spectra during cathodic sweep in 1 M KOH+$Ca(OH)_2$ (sat'd) electrolyte continuously sparged with Ar with 10 mM BTA (**a**), 10 mM Pz (**b**), and 10 mM EA (**c**)

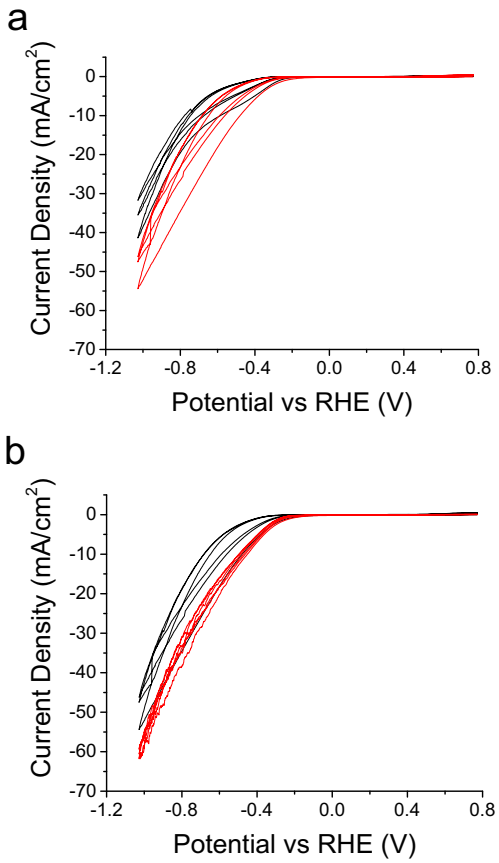

Fig. 4 Cyclic voltammetry (50 mV/s) of Au in 1 M KOH+Ca $(OH)_2$ (sat'd) saturated with CO_2 (pH approximately 7.8) **a** with (*red*) and without (*black*) EA and **b** with EA at 0 rpm (*black*) and without EA at 1600 rpm (*red*)

Electrochemistry with adsorbed N-containing compounds

Figure 4 shows cyclic voltammetry of a Au disk in a CO_2-saturated electrolyte with a pH of ca. 7.8. As shown in Fig. 4a when EA is cast on the Au surface, the maximum current is increased, but the onset is unaffected in the first cycle. The current density magnitude increases, when EA is added to the Au surface, by a factor of approximately 1.3 at low overpotentials (ca. −0.4 to −0.5 V vs. RHE) and approximately 1.6 at higher overpotentials. Tafel analysis revealed a larger slope of approximately 198 mV/decade in the low overpotential regime compared to the 120 mV/decade found for bare Au discussed above. As the EA/Au system was cycled, the activity decayed towards that of bare Au, suggesting that the EA was not strongly bound to the Au surface. Figure 4b compares cyclic voltammetry for a stationary Au disk onto which EA has been adsorbed and a rotated, bare Au disk (absent EA). Interestingly, the current obtained from the first cycle of the ethanolamine-coated Au electrode compares well to the current achieved at a rotated Au electrode during CO_2 reduction. As expected, neither Au electrode exhibits rotation rate dependence (not shown).

Conclusions

The SER spectra collected during CO_2 reduction on Au only exhibit a peak associated with CO, adsorbed on atop sites, when N-containing additives such as BTA or EA are present in the electrolyte. These additives do not affect the CO_2 reduction activity or product distribution of the Au electrodes. As noted previously, this is in contrast to their effect on Ag electrodes, where the N-containing additives lead to enhanced CO production. On Ag, CO formed was only weakly adsorbed on the Ag surface and that weaker adsorption was encouraged by the addition of an additive. Thus, on Ag, the role of the additive is to further destabilize the adsorbed CO. We noted that CO adsorption on Au is much weaker than that on Ag (ca. 0.28 eV vs. ca. 0.40 eV, respectively) [23–26]. So, on Au, the CO product is already destabilized which is why the additives demonstrate no effect on CO_2 reduction.

In contrast, by adding a known CO_2 scavenger, EA, we can enhance the CO_2 reduction rate to CO, at least during initial cycles. This enhancement is approximately the same magnitude as that found with electrode rotation. The change in current density indicates that CO_2 association to the EA/Au system improves by a factor of approximately 1.3 at low overpotentials (ca. −0.4 to 0.5 V vs. RHE) and approximately 1.6 at high overpotentials, which demonstrates that the adsorbed EA additive increases the CO_2 activity near the Au electrode surface. Overall, the enhancement suggests that the origin of the enhancement is the increased availability of the CO_2 reactant at the Au surface.

In summary, on Au electrodes, the CO product is already sufficiently destabilized to be easily removed and increasing the concentration, and thus the availability, of the CO_2 reactant near the Au surface yields an enhancement in the CO_2 reduction activity. Therefore, enhancing CO_2 reduction to CO on Au should focus primarily on the reactant side of the Sabatier plot as the product, CO, is already sufficiently destabilized. As demonstrated, this can be achieved utilizing various N-containing additives that serve to stabilize or concentrate the CO_2 reactant near the Au surface.

Acknowledgments The authors acknowledge the National Science Foundation (NSF) for support of this research.

References

1. Appel AM, Bercaw JE, Bocarsly AB, Dobbek H, DuBois DL, Dupuis M, Ferry JG, Fujita E, Hille R, Kenis PJA, Kerfeld CA, Morris RH, Peden CHF, Portis AR, Ragsdale SW, Rauchfuss TB, Reek JNH, Seefeldt LC, Thauer RK, Waldrop GL (2013) Chem Rev 113(8):6621–6658
2. Whipple DT, Kenis PJA (2010) J Phys Chem Lett 1(24):3451–3458
3. Olah GA, Prakash GKS, Goeppert A (2011) J Am Chem Soc 133(33):12881–12898
4. Fu Q, Mabilat C, Zahid M, Brisse A, Gautier L (2010) Energy Environ Sci 3(10):1382–1397
5. Hori Y (2008) Electrochemical CO2 Reduction on metal electrodes. In: Vayenas CG, White RE, Gamboa Aldeco ME (eds) Modern aspects of electrochemistry, No 42. Modern aspects of electrochemistry, vol 42. pp 89-189
6. Noda H, Ikeda S, Oda Y, Imai K, Maeda M, Ito K (1990) Bull Chem Soc Jpn 63(9):2459–2462
7. Christophe J, Doneux T, Buess-Herman C (2012) Electrocatalysis 3(2):139–146
8. Ishimaru S, Shiratsuchi R, Nogami G (2000) J Electrochem Soc 147(5):1864–1867
9. Hansen HA, Varley JB, Peterson AA, Norskov JK (2013) J Phys Chem Lett 4(3):388–392
10. Noda H, Ikeda S, Yamamoto A, Einaga H, Ito K (1995) Bull Chem Soc Jpn 68(7):1889–1895
11. Hori Y, Murata A, Kikuchi K, Suzuki S (1987) J Chem Soc Chem Commun 10:728–729
12. Delacourt C, Ridgway PL, Newman J (2010) J Electrochem Soc 157(12):B1902–B1910
13. Chen Y, Li CW, Kanan MW (2012) J Am Chem Soc 134(49): 19969–19972
14. Kaneco S, Iiba K, Ohta K, Mizuno T, Saji A (1998) J Electroanal Chem 441(1-2):215–220
15. Perez ER, Garcia JR, Cardoso DR, McGarvey BR, Batista EA, Rodrigues-Filho UP, Vielstich W, Franco DW (2005) J Electroanal Chem 578(1):87–94
16. Christensen PA, Hamnett A, Muir AVG, Freeman NA (1990) J Electroanal Chem 288(1-2):197–215
17. Tornow CE, Thorson MR, Ma S, Gewirth AA, Kenis PJA (2012) J Am Chem Soc 134(48):19520–19523
18. Schmitt KG, Gewirth AA (2014) J Phys Chem C 118(31):17567–17576
19. Thorum MS, Anderson CA, Hatch JJ, Campbell AS, Marshall NM, Zimmerman SC, Lu Y, Gewirth AA (2010) J Phys Chem Lett 1(15): 2251–2254
20. Gao P, Gosztola D, Leung LWH, Weaver MJ (1987) J Electroanal Chem 233(1-2):211–222
21. Cooney RP, Mahoney MR, Howard MW (1980) Chem Phys Lett 76(3):448–452
22. Schultz ZD, Feng ZV, Biggin ME, Gewirth AA (2006) J Electrochem Soc 153(2):C97–C107
23. Abild-Pedersen F, Andersson MP (2007) Surf Sci 601(7):1747–1753
24. Gajdos M, Eichler A, Hafner J (2004) J Phys-Cond Matt 16(8): 1141–1164
25. Santiago-Rodriguez Y, Herron JA, Curet-Arana MC, Mavrikakis M (2014) Surf Sci 627:57–69
26. McElhiney G, Papp H, Pritchard J (1976) Surf Sci 54(3):617–634
27. Yang H, Xu Z, Fan M, Gupta R, Slimane RB, Bland AE, Wright I (2008) J Environ Sci (China) 20(1):14–27
28. Lu Q, Rosen J, Zhou Y, Hutchings GS, Kimmel YC, Chen JG, Jiao F (2014). Nat Commun 5
29. Lee S, Ju H, Machunda RL, Uhm S, Lee JK, Lee HJ, Lee J (2014) J Mater Chem A.
30. Schmidt TJ, Gasteiger HA, Behm RJ (1999) J Electrochem Soc 146(4):1296–1304
31. Gojkovic SL, Gupta S, Savinell RF (1999) J Electroanal Chem 462(1):63–72
32. Kapalka A, Foti G, Comninellis C (2008) Electrochem Commun 10(4):607–610
33. Medard C, Lefevre M, Dodelet JP, Jaouen F, Lindbergh G (2006) Electrochim Acta 51(16):3202–3213
34. Kudelski A, Pettinger B (2004) Chem Phys Lett 383(1-2):76–79
35. Kudelski A (2009) J Solid State Electrochem 13(2):225–230
36. Beltramo GL, Shubina TE, Koper MTM (2005) ChemPhysChem 6(12):2597–2606
37. Blizanac BB, Arenz M, Ross PN, Markovic NM (2004) J Am Chem Soc 126(32):10130–10141
38. Blizanac BB, Lucas CA, Gallagher ME, Arenz M, Ross PN, Markovic NM (2004) J Phys Chem B 108(2):625–634
39. Krishnakumar V, Jayamani N, Mathammal R (2011) Spectrochim Acta Part -Molec Biomolec Spectroscop 79(5):1959–1968
40. Thomas S, Venkateswaran S, Kapoor S, D'Cunha R, Mukherjee T (2004) Spectrochim Acta Part -Molec Biomolec Spectroscop 60(1-2):25–29